

Oxidation of 4-Methoxy-1-Naphthol on Promoted Platinum Catalysts¹

M. V. Maphoru^a, J. Heveling^{a, b, *}, and S. Kesavan Pillai^c

^aDepartment of Chemistry, Tshwane University of Technology, Pretoria 0001, South Africa

^bInstitute for Nano-Engineering Research, Tshwane University of Technology, Pretoria 0001, South Africa

^cNational Centre for Nano-Structured Materials, Council for Scientific and Industrial Research, Pretoria 0001, South Africa

*e-mail: hevelingj@tut.ac.za

Received October 24, 2016

Abstract—Oxidative coupling of naphthols is a useful method for the formation of new carbon-carbon bonds in organic synthesis. In the presence of hydrogen peroxide, platinum supported on activated carbon catalyses this reaction. The outcome is influenced by the solvent, the reaction temperature and the physical structure of the catalyst. The catalyst structure is determined by the synthesis method and the modifier used (Bi or Sb). Within 40 min 4-methoxy-1-naphthol can be converted to 4,4'-dimethoxy-2,2'-binaphthalenyl-1,1'-diol with a yield of up to 94%, or to 4,4'-dimethoxy-2,2'-binaphthalenylidene-1,1'-dione with a yield of 92%. High amounts of quinoid byproducts ($\leq 22\%$) are observed in nitromethane as the solvent.

Keywords: oxidative coupling, 1-naphthol, platinum, promoter, solvent effect, selectivity

DOI: 10.1134/S0023158417040103

INTRODUCTION

Aryl-aryl bond formations are of great importance in synthetic organic chemistry. The oxidative coupling of naphthols can be used for this purpose. Takeya et al. [1, 2] found that 4-methoxy-1-naphthol (**1**) couples in the presence of oxygen and semiconductors, e.g. SnO₂ and ZrO₂, to give the binaphthol **2**, the binaphthone **3** and the coupled naphthoquinone **4** (see the scheme). These compounds are of importance for the pharmaceutical industry [1, 2]. They are also useful intermediates for the preparation of naturally occurring substances, such as diosindigo B, biramentaceone, and violet-quinone [1]. Based on an earlier patent [3], we recently reported the effective use of Bi-promoted Pt supported on activated carbon (AC, 5%Pt–5%Bi/AC) as a heterogeneous catalyst for the oxidative coupling of substituted 1-naphthols that contain electron-donating groups in *ortho*- or *para*-position to the hydroxyl group [4]. Pt–Bi/AC is a commercially available catalyst for electrocatalysis and selective oxidation reactions. With respect to the latter application, it is speculated that Bi exerts a geometric blocking effect on Pt, thus decreasing the active site ensembles of Pt. These minimised sites still allow for the desired chemical reaction to proceed, but they are inactive for unwanted side reactions [5, 6]. Lately, we demonstrated that antimony can be used to a similar effect, and 5%Pt–5%Sb/AC was shown to have superior selectivity for the oxidation of cinnamyl alcohol to cinnamaldehyde in comparison to corresponding Bi-containing catalysts [7].

AC supported metal catalysts can be prepared with the help of chemical and physical methods. Chemical methods include impregnation and electroless (reductive) deposition. Physical methods make use of lasers, sonication, microwave (MW) and UV irradiation, as well as plasma technology and supercritical fluids [8]. The method of preparation has a decisive influence on the structure and the morphology of the final product [9]. Most deposition methods result in an extended particle-size distribution, accompanied by agglomeration [8]. In contrast, use of MW irradiation during synthesis can be expected to create homogeneous nucleation sites, resulting in a narrowed particle-size distribution, high metal dispersion, and uniform particle shapes [10, 11]. In addition, MW irradiation offers shorter reaction times and reduced energy consumption [10, 12]. In combination with ethylene glycol it is a very convenient, fast and efficient method of metal deposition onto supports [13], as glycol can act both as the solvent and as the reducing agent for metal precursors [14].

In this study, the catalytic properties of 5%Pt–5%Bi/AC and 5%Pt–5%Sb/AC catalysts prepared by electroless (reductive) deposition (ED), including MW assisted glycol reduction, are described. The nanostructures obtained have an influence on the catalytic activity and selectivity for the oxidative coupling of 4-methoxy-1-naphthol, which is used as the substrate.

EXPERIMENTAL

Materials

Antimony chloride (99%) was purchased from Sigma-Aldrich and ethylene glycol (99.5%) from Pro-

¹ The article is published in the original.

mark Chemicals. All other materials were as listed in a previous publication [15]. The purity of 4-methoxy-1-naphthol was 97% (Sigma-Aldrich).

Synthesis of Catalysts

The preparation of 5%Pt–5%Bi on AC by ED was carried out as described earlier [15]. By testing with AgNO_3 , the final aqueous filtrate was found to be free of chloride. Vacuum-dried (VD) samples were dried at room temperature (r. t.) under vacuum for 4 h, oven-dried (OD) samples in an oven at 140°C for 24 h. The same procedure was used to prepare VD 5%Pt/AC, as well as VD and OD 5%Pt–5%Sb/AC; SbCl_3 (0.1228 g, 0.4108 mmol) was the Sb precursor.

Microwave-assisted loading (MW): for the preparation of MW 5%Pt–5%Bi/AC, $\text{H}_2\text{PtCl}_6 \cdot 6\text{H}_2\text{O}$ (0.1328 g, 0.2564 mmol) and $\text{Bi}(\text{NO}_3)_3 \cdot 5\text{H}_2\text{O}$ (0.1161 g, 0.2393 mmol) were transferred into a 100 mL beaker containing ethylene glycol (20 mL), followed by ultrasonication for 10 min to completely dissolve the salts. To this mixture, AC (0.9001 g) was added, followed by ultrasonication for 1 h prior to MW irradiation. The MW-assisted metal loading was conducted in a Mars Xpress MW system at 600 W and 190°C in a closed Teflon vessel. The time to reach the final temperature was set at 5 min, and irradiation continued for 10 min at 190°C to allow for the complete reduction of Pt(IV) to Pt(0). Samples were centrifuged, washed with deionised water, and left to air-dry (AD) for 24 h. The same method was followed to prepare MW 5%Pt–5%Sb/AC; SbCl_3 (0.1228 g, 0.4111 mmol) was used as the precursor for Sb.

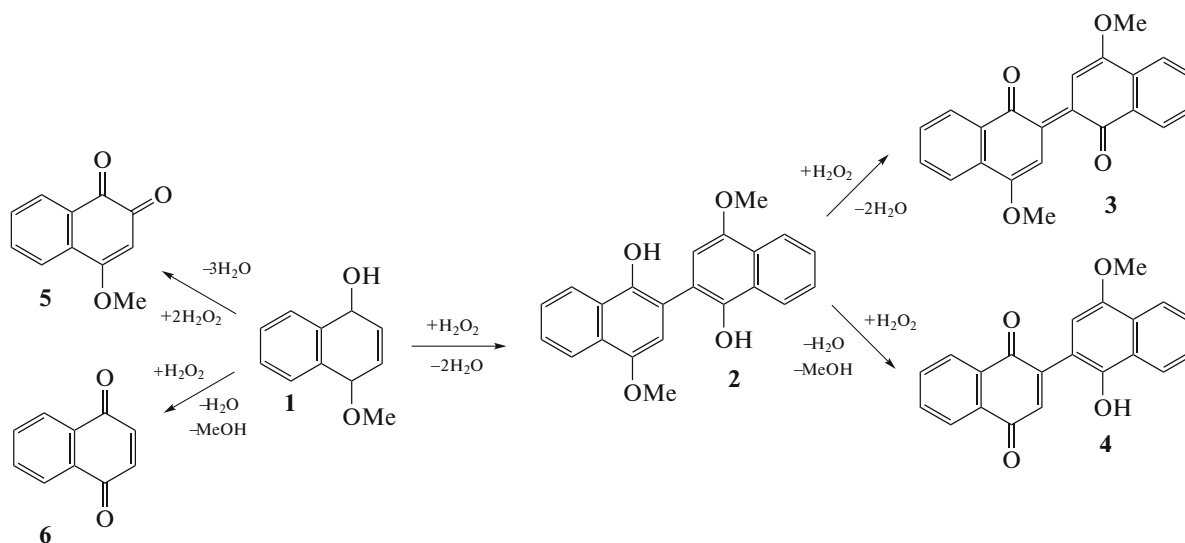
Characterization of Nanocomposites and Organic Compounds

Elemental analyses (Pt, Bi and Sb) were performed on a Spectro Arcos FHS ICP-OES instrument. Nitro-

gen physisorption (BET) was carried out using a Micro-metrics ASAP 2020 surface area and porosity analyser. Approximately 0.05 g of each sample was degassed for 6 h and analysed at -196°C (77 K) for 5 h using N_2 as the adsorbent. Sample morphologies and elementary compositions were analysed by means of a JEOL JSM-7500F field-emission scanning electron microscope with an electron accelerating voltage of 15.0 kV. All samples were sputter coated with carbon. High-resolution transmission electron microscopy (HRTEM) was performed on a JEOL JEM-2100 HRTEM instrument. The electron acceleration voltage was 200 kV. The samples were dispersed in ethanol using an ultrasonic bath, and supported on carbon-coated copper grids (200 mesh). Particle sizes were measured with the help of the ImageJ software. Approximately 100 particles were measured per sample. The full characterization of the organic compounds was described previously [15].

Oxidation Reactions and Product Separation

Oxidative coupling reactions (at r. t. or under reflux) were carried out in the same manner as described earlier [15]. That is, for each reaction 6.34 mmol starting material (SM) and 0.0401 g catalyst were used in 25 mL of solvent, to which 22.1 mmol H_2O_2 was added as a 30% aq. solution over 40 min. The reaction mixture was separated by column chromatography. Product selectivities were calculated as mole percentages based on the moles of SM incorporated into each product. Turn-over frequencies (TOFs) are reported as moles of H_2O_2 required for the formation of all identified products (compare Scheme 1) per moles of platinum present in the catalyst over the total reaction time (min^{-1}).



Scheme 1. Oxidation of 4-methoxy-1-naphthol (**1**) over Pt catalysts; H_2O_2 is the oxidant.

Table 1. Preparation methods, drying conditions, metal loadings, surface areas and average particle sizes of samples

Sample	Sample designation	Preparation method	Drying method	Drying <i>T</i> , °C	Drying <i>t</i> , h	Pt	Bi	Sb	<i>S</i> , m ² g ⁻¹	APS ^a , nm
						wt %				
AC	AC	–	–	–	–	–	–	–	1195	–
VD 5%Pt/AC	VD Pt	ED	VD	r. t.	4	5.0	–	–	865	39.7
VD 5%Pt–5%Bi/AC	VD Bi	ED	VD	r. t.	4	4.9	4.8	–	655	8.75
OD 5%Pt–5%Bi/AC	OD Bi	ED	OD	140	24	4.9	4.9	–	535	3.26
MW 5%Pt–5%Bi/AC	MW Bi	MW	AD	r. t.	24	5.0	4.9	–	860	6.96
VD 5%Pt–5%Sb/AC	VD Sb	ED	VD	r. t.	4	5.0	–	4.8	625	–
OD 5%Pt–5%Sb/AC	OD Sb	ED	OD	140	24	4.8	–	4.8	620	–
MW 5%Pt–5%Sb/AC	MW Sb	MW	AD	r. t.	24	5.0	–	4.9	855	8.32

^a Determined by HRTEM.

RESULTS AND DISCUSSION

Catalyst Characterization

The sample designations, the preparation methods, the drying conditions, the surface areas and the average particle sizes (APS) measured for the different catalysts are shown in Table 1. Independent of the synthesis method used, the metal loadings are always near to the targeted values. The BET surface area of the AC support is close to 1200 m²/g. Lower total surface areas are found after metal loading, probably due to some pore blockage. Some restructuring of AC must also be taken into consideration. Zhu and others [16] observed the exfoliation of graphite by MW treatment, accompanied by a considerable increase in surface area. Similarly, our composites prepared by the MW method distinguish themselves by high remaining surface areas (855–860 m²/g).

HRTEM images of the Bi- and Sb-promoted catalysts are shown in Fig. 1. From these the APS (Table 1) were determined. The APS for VD Bi (Fig. 1a) is 8.75 nm. The nanoparticles of OD Bi (Fig. 1b) are highly dispersed and have an APS of 3.26 nm. Small particles are possibly more effective in blocking some of the accessible pores of the AC support. Accordingly, OD Bi has the lowest surface area (535 m²/g) of all the materials seen in Table 1. The APS of MW Bi (Fig. 1c) is 6.96 nm. The unpromoted VD Pt has by far the highest APS (39.7 nm) and also the highest total surface area of all metal-loaded samples.

For VD Sb (Fig. 1d) agglomerated chain-like structures with a diameter of ~11.6 nm are observed. No fringes were detectable. HRTEM-EDX analysis (Fig. 2) indicates that the nanochains contain both Pt and Sb. This was also confirmed by SEM “point and shoot” EDX analysis (not shown). The measurements suggest the presence of almost amorphous Pt embedded in amorphous Sb or vice versa, thus forming a nearly amorphous matrix. For carbon-supported Pt–Sb, also Yu and Pickup [17] found that Pt and Sb are always associated. The morphology of OD Sb is

similar and a chain-like morphology emerges by HRTEM (Fig. 1e); as for VD Sb, the nanochains were also found to contain both Pt and Sb. Due to this peculiar morphology, particle-size distributions could not be determined (Table 1). For MW Sb (Fig. 1f) uniform crystalline cubic particles containing Pt and Sb are seen, and an APS of 8.32 nm was calculated.

Oxidative Coupling of 4-Methoxy-1-Naphthol

Hydrogen peroxide was used as the oxidant. Ideally, the addition rate of the oxidant should match the rate of its consumption [18], as any excess of H₂O₂ must be expected to decompose on the catalyst surface [19, 20] and may lead to the over-oxidation of the catalytically active metal (Pt) [6]. For each test, 3.5 equivalents of the oxidant were added in a drop-wise manner over 40 min, which was sufficient to achieve total conversions over the catalyst with the highest Pt dispersion (OD Bi) at r. t. and under reflux. This is of significance, because the catalyst with the highest Pt surface area must also be expected to exhibit the highest decomposition rate for H₂O₂. Anderson et al. [18] needed more than 5 equivalents of H₂O₂ to completely convert 1-octanol over a 5%Pt–1%Bi/C catalyst. Remarkably, the need for excess H₂O₂ is not a peculiarity of precious metal catalysts, e.g. Kholdeeva et al. [21] used a 2.5-fold excess for an oxidation reaction catalysed by Ti-silicate.

Under our reaction conditions 4,4-dimethoxy-2,2'-binaphthalenyl-1,1'-diol (binaphthol **2**) and 4,4'-dimethoxy-2,2'-binaphthalenylidene-1,1'-dione (Rus-sig's blue or binaphthone **3**) are always the major products, accompanied by variable amounts of quinones, namely 1'-hydroxy-4'-methoxy-2,2'-binaphthalenyl-1,4-dione (coupled naphthoquinone **4**), 4-methoxy-1,2-naphthoquinone **5**, and 1,4-naphthoquinone **6** (Scheme 1). The binaphthol must be regarded as the intermediate to **3** and **4** [4]. The conversions and selectivities obtained over our catalysts in different solvents (at r. t. or under reflux) are listed in

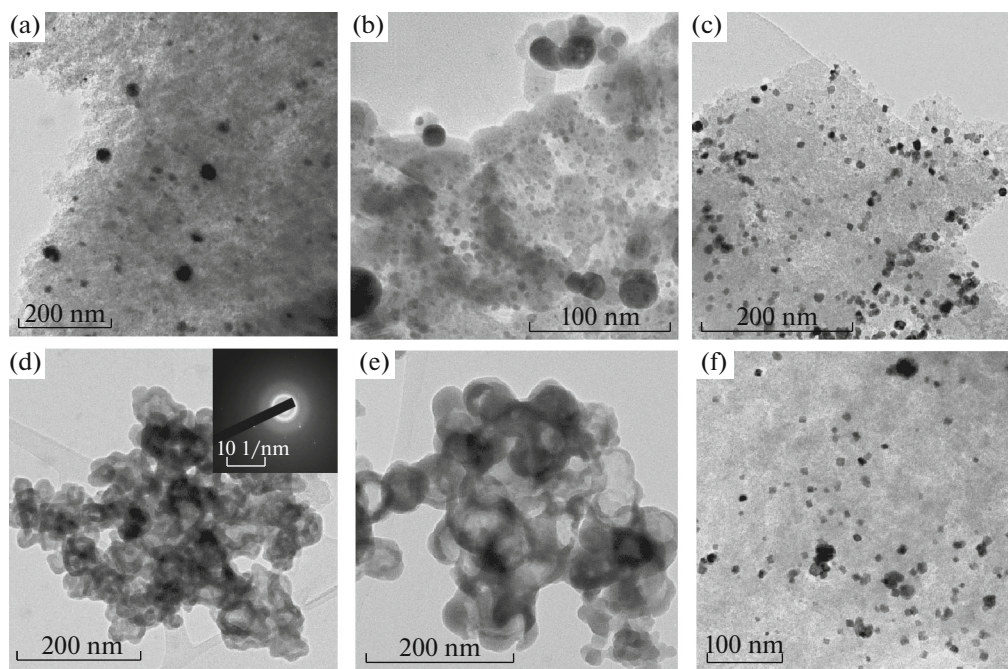


Fig. 1. HRTEM images of VD Bi (a), OD Bi (b), MW Bi (c), VD Sb (d), OD Sb (e), and MW Sb (f).

Table 2. The TOFs are plotted in Fig. 3. These are based on the total amount (mol) of Pt present on each catalyst. Under comparable reaction conditions, this should lead to TOFs reflecting the relative activities of the catalysts [22, 23].

Judged by the TOFs, the catalyst activity in MeNO₂ at r. t. increases in the order OD Sb < VD Sb < VD Pt < MW Bi \cong MW Sb = VD Bi < OD Bi (Fig. 3). Only over the most active catalyst is **6** observed as a byproduct (Table 2, entry 3). Under reflux (entries 8–14) conversions are complete for all catalysts, and **2** is quantita-

tively converted further to the binaphthone **3**. In this regard, OD Sb (entry 13) is the only exception (93% conv.); it is also the only catalyst that does not form any **3** and **6**. As a rule, high amounts of quinones are observed in MeNO₂.

In THF at 60°C the reaction is very selective and no quinones are formed (entries 15–21). Depending on the catalyst composition, the conversion increases up to 100% and increasing amounts of **2** are converted further to **3**. The TOFs (Fig. 3) improve in the order OD Sb < VD Sb < VD Bi < MW Sb < OD Bi \cong MW Bi \cong VD Pt.

In CH₂Cl₂ at 38°C (entries 22–28) OD Bi appears to be the most active catalyst (entry 24); it gives 100% conversion of **1**, and **2** is completely converted to **3**. However, some **4** (17.4%) and a high amount of unidentified side products (15.6%) are also found. Therefore, based on the calculation of the TOFs, the order of reactivity is as follows: OD Sb < VD Sb < VD Bi \cong VD Pt < OD Bi < MW Sb \cong MW Bi. Like in THF, the naphthoquinones **5** and **6** are not formed.

Figure 3 clearly demonstrates that VD and OD Sb under all conditions are the two least active catalysts, while VD Bi, MW Bi and MW Sb show a rather similar performance. At least in MeNO₂ at r. t. (first set of plots in Fig. 3) OD Bi stands out as the most active sample. In this set all catalysts are compared at partial conversion with respect to **1** and **2**, a condition that is preferable for the meaningful comparison of catalysts.

The structures of VD and OD Sb differ profoundly from all the other samples. Both consist of agglomerated Pt–Sb nanochains (Figs. 1d, 1e) and have similar

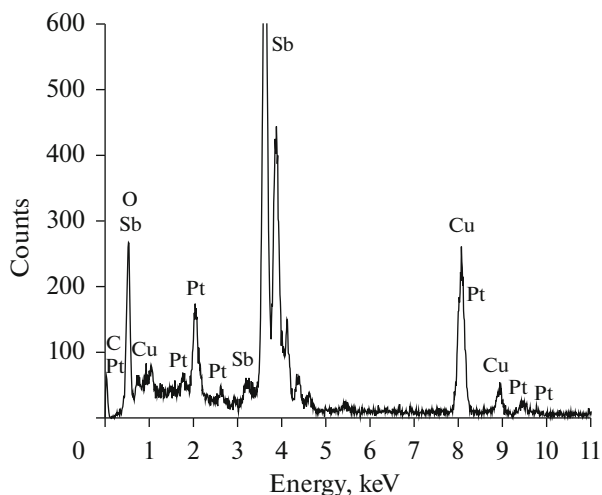


Fig. 2. HRTEM-EDX spectrum of the VD Sb nanochains seen in Fig. 1d.

Table 2. Oxidation of 4-methoxy-1-naphthol catalysed by AC supported 5%Pt, 5%Pt–5%Bi and 5%Pt–5%Sb catalysts prepared by different methods

Entry	Catalyst	Solvent	T, °C	Conv., %	Selectivity, mol %				
					2	3	4	5	6
1	VD Pt	MeNO ₂	r. t.	33.1	36.9	61.3	–	–	–
2	VD Bi	MeNO ₂	r. t.	54.1	37.3	59.9	–	–	–
3 ^a	OD Bi	MeNO ₂	r. t.	100	7.2	55.5	–	–	16.9
4	MW Bi	MeNO ₂	r. t.	47.8	25.3	73.8	–	–	–
5 ^b	VD Sb	MeNO ₂	r. t.	31.4	76.8	–	–	–	–
6	OD Sb	MeNO ₂	r. t.	3.4	61.8	–	–	–	–
7	MW Sb	MeNO ₂	r. t.	53.3	35.3	64.0	–	–	–
8 ^c	VD Pt	MeNO ₂	96	100	Trace	74.0	–	–	15.8
9	VD Bi	MeNO ₂	96	100	–	88.4	–	Trace	7.0
10 ^a	OD Bi	MeNO ₂	96	100	–	67.1	–	1.3	20.7
11	MW Bi	MeNO ₂	96	100	–	83.1	–	Trace	12.8
12 ^c	VD Sb	MeNO ₂	96	100	–	63.4	–	Trace	18.0
13 ^a	OD Sb	MeNO ₂	96	93.2	74.2	–	–	7.4	–
14	MW Sb	MeNO ₂	96	100	–	82.0	–	Trace	11.7
15 ^c	VD Pt	THF	60	97.0	2.3	95.2	Trace	–	–
16 ^c	VD Bi	THF	60	94.0	20.5	64.4	–	–	–
17	OD Bi	THF	60	100	14.0	81.0	–	–	–
18	MW Bi	THF	60	100	15.0	84.9	–	–	–
19	VD Sb	THF	60	≤100	93.5	Trace	–	–	–
20	OD Sb	THF	60	6.2	93.7	–	–	–	–
21	MW Sb	THF	60	100	35.2	63.1	–	–	–
22	VD Pt	CH ₂ Cl ₂	38	92.7	41.2	58.1	–	–	–
23	VD Bi	CH ₂ Cl ₂	38	100	58.1	41.3	–	–	–
24 ^a	OD Bi	CH ₂ Cl ₂	38	100	Trace	67.0	17.4	–	–
25	MW Bi	CH ₂ Cl ₂	38	100	8.1	91.6	–	Trace	–
26	VD Sb	CH ₂ Cl ₂	38	61.0	98.9	–	–	–	–
27	OD Sb	CH ₂ Cl ₂	38	6.8	92.5	–	–	–	–
28	MW Sb	CH ₂ Cl ₂	38	100	18.1	81.6	–	Trace	–

^a A violet-blue compound that appears to be a polymer was detected (¹³C NMR), together with other byproducts.^b Polymeric compounds and black deposits formed.^c Two unknown compounds (purple green) with similar retention factors could not be separated by column chromatography.

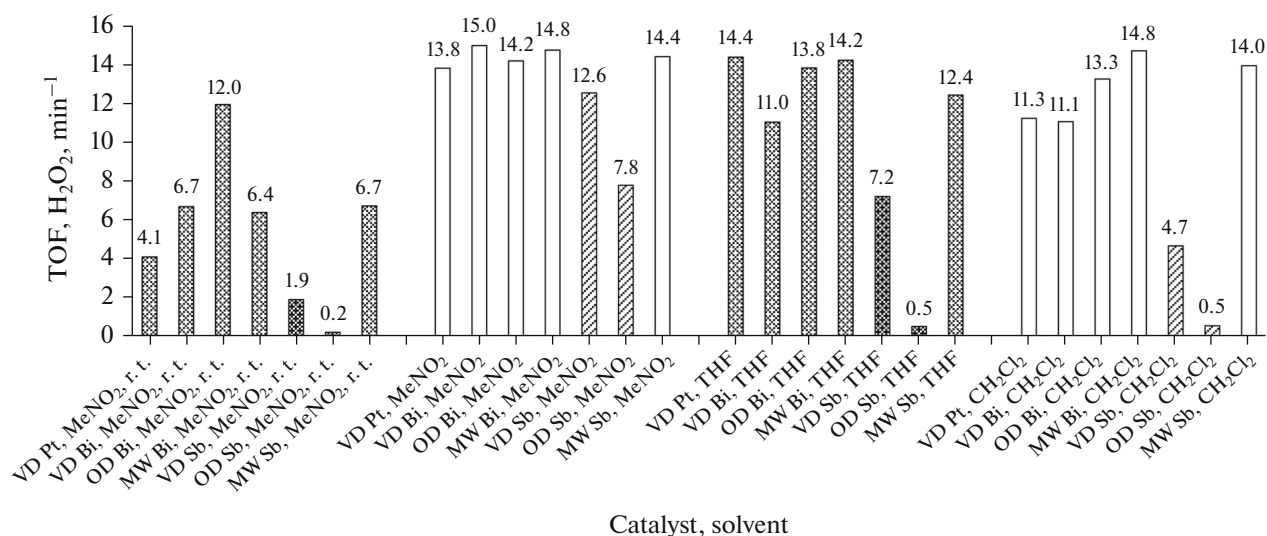


Fig. 3. TOFs based on the productive consumption of H₂O₂, calculated for the catalysts used in different solvents (r. t. or reflux).

total surface areas (Table 1). Fringes could not be detected by HRTEM, suggesting that amorphous Sb covers Pt. However, some exposed Pt metal was detected by SAED (insert of Fig. 1d). It is conceivable, that all the materials other than VD and OD Sb are catalytically more active because of a higher presence of surface Pt. The differences in activity and selectivity of the catalysts, as seen in Table 2 and Fig. 3, can therefore be attributed to variations in the nanostructure, as well as variations in the metal distribution and exposure. The APS of VD Bi, MW Bi and MW Sb are relatively close to each other (7.0–8.8 nm, Table 1), an observation that may significantly contribute to their similarity in catalytic performance. In contrast, on OD Bi platinum is highly dispersed (APS = 3.3 nm), and this catalyst exhibits by far the highest TOF (12 min⁻¹) when compared to the other samples under the condition of partial conversion in MeNO₂ at r. t. (Fig. 3). As should be expected, the activity of VD Pt (APS = 39.7 nm) is rather low, and at r. t. in MeNO₂ it shows a TOF of only 4.1 min⁻¹.

It was shown earlier [15] that the (most active) OD Bi catalyst can be recycled without any significant decline in activity, but metal losses of 2.6% (Pt) and 5.1% (Bi) occurred during the first run. In a control test no catalytic activity of leached metal was found.

The results obtained are in agreement with the previously proposed mechanism, by which the reaction proceeds on metallic-state platinum [4].

As to the effect of the solvent, it can be stated that THF does not promote the formation of quinones, and high yields of **2** can be obtained (93.5%). However, in MeNO₂ quinones are formed in significant quantities. In a dedicated study [15], we could not establish a positive correlation between reactivity data and the solvent donor number (DN) [24]. Such a rela-

tionship could be expected for an oxidation reaction, but Takeya et al. [25] noticed that for SnCl₄-mediated oxidative coupling reactions of 1-naphthol, solvents with a low DN were more favourable. Nevertheless, in our case the selectivity to the coupled products **2** and **3** was found to correlate negatively with the solvent acceptor number; no other correlations between solvent properties and reaction data could be established [15].

CONCLUSIONS

Platinum is an efficient catalyst for the oxidative coupling of **1**. At complete conversion of the SM, high selectivities to the binaphthone **3** can be obtained over MW Bi in THF (85%) and in CH₂Cl₂ (92%). Over the less active VD Sb catalyst the intermediate binaphthol **2** is formed as the principal product in THF (94%). No quinoidal side products are found in THF. The highest amounts of quinones are seen in MeNO₂: over OD Bi 17% of **6** are formed at r. t. and 21% under reflux.

The activity and selectivity of the catalysts is strongly influenced by their structural and morphological characteristics. These vary with the catalyst synthesis method and the promoter element used (Bi or Sb). VD and OD Sb are characterized by a chain-like morphology of Sb and Pt with little exposure of Pt crystals. Under all reaction conditions, these two samples are of low activity. The highest activity is indicated for OD Bi, which contains Pt in a well dispersed state. This sample shows always maximum conversions of **1** and **2**.

The results obtained are in agreement with a previously proposed mechanism, by which the reaction proceeds on metallic-state platinum.

Ongoing work involves further characterization of the catalysts and testing of other SMs.

ACKNOWLEDGMENTS

M.V. Maphoru is grateful for a DAAD-NRF bursary.

REFERENCES

1. Takeya, T., Otsuka, T., Okamoto, I., and Kotani, E., *Tetrahedron*, 2004, vol. 60, p. 10681.
2. Otsuka, T., Okamoto, I., Kotani, E., and Takeya, T., *Tetrahedron Lett.*, 2004, vol. 45, p. 2643.
3. US Patent 149285, 2003.
4. Maphoru, M.V., Heveling, J., and Pillai, S.K., *ChemPlusChem*, 2014, vol. 79, p. 99.
5. Mallat, T., Bodnar, Z., Hug, P., and Baiker, A., *J. Catal.*, 1995, vol. 153, p. 131.
6. Mallat, T. and Baiker, A., *Chem. Rev.*, 2004, vol. 104, p. 3037.
7. Langa, S., Nyamunda, B.C., and Heveling, J., *Catal. Lett.*, 2016, vol. 146, p. 755.
8. Campelo, J.M., Luna, D., Luque, R., Marinas, J.M., and Romero, A.A., *ChemSusChem*, 2009, vol. 2, p. 18.
9. Amin, R.S., Elzatahry, A.A., El-Khatib, K.M., and Elsayed Youssef, M., *Int. J. Electrochem. Sci.*, 2011, vol. 6, p. 4572.
10. Wu, Z., Borretto, E., Medlock, J., Bonrath, W., and Cravotto, G., *ChemCatChem*, 2014, vol. 6, p. 2762.
11. Chen, W., Zhao, J., Lee, J.Y., and Liu, Z., *Mater. Chem. Phys.*, 2005, vol. 91, p. 124.
12. Ko, F., Lee, C., Ko, C., and Chu, T., *Carbon*, 2005, vol. 43, p. 727.
13. Li, H., Zhang, S., Yan, S., Lin, Y., and Ren, Y., *Int. J. Electrochem. Sci.*, 2013, vol. 8, p. 2996.
14. Kawasaki, H., *Nanotechnol. Rev.*, 2013, vol. 2, p. 5.
15. Maphoru, M.V., Heveling, J., and Kesavan Pillai, S., *Eur. J. Org. Chem.*, 2016, p. 331.
16. Zhu, Y., Murali, S., Stoller, M.D., Velamakanni, A., Piner, R.D., and Ruoff, R.S., *Carbon*, 2010, vol. 48, p. 2118.
17. Yu, X. and Pickup, P.G., *Electrochim. Acta*, 2010, vol. 55, p. 7354.
18. Anderson, R., Griffin, K., Johnston, P., and Alsters, P.L., *Adv. Synth. Catal.*, 2003, vol. 345, p. 517.
19. Kreja, L., *Z. Phys. Chem.*, 1984, vol. 140, p. 247.
20. Hasnat, M.A., Rahman, M.M., Borhanuddin, S.M., Siddiqua, A., Bahadur, N.M., and Karim, M.R., *Catal. Commun.*, 2010, vol. 12, p. 286.
21. Kholdeeva, O.A., Zalomaeva, O.V., Shmakov, A.N., Melgunov, M.S., and Sorokin, A.B., *J. Catal.*, 2005, vol. 236, p. 62.
22. Kozuch, S. and Martin, J.M.L., *ACS Catal.*, 2012, vol. 2, p. 2787.
23. Lente, G., *ACS Catal.*, 2013, vol. 3, p. 381.
24. Gutmann, V., *Electrochim. Acta*, 1976, vol. 21, p. 661.
25. Takeya, T., Doi, H., Ogata, T., Otsuka, T., Okamoto, L., and Kotani, E., *Tetrahedron*, 2004, vol. 60, p. 6295.